HYBRID BACKSTEPPING CONTROL OF A DOUBLY FED WIND ENERGY INDUCTION GENERATOR

ROUABHI Riyadh [a,*], ABDESSEMED Rachid [a], CHOUDER Aissa [b], DJERIOUI Ali [b]

(a) LEB – Research Laboratory, Department of Electrical Engineering, Batna University, 05000 Batna, Algeria
(b) Department of Electrical Engineering, Faculty of Technology, University of M'sila, Algeria

ABSTRACT

In this paper, hybrid control strategy applied to doubly fed induction generator (DFIG) used in wind energy conversion systems (WECS) is presented. The main objective of the study is to derive a control strategy which will be applied to a bidirectional converter supplying a DFIG based on the combination of vector and backstepping control. Vector control approach has been initially carried out in order to get a decoupled active and reactive power with proportional-integral compensator (PI). In order to enhance some of the drawbacks of the PI compensator in terms of robustness, transient response and steady state error a backstepping approach has been used. Simulation study carried out on the DFIG generating both real powers extracted from the turbine and the required reactive power have shown good performances compared to those obtained by using PI compensator for the overall expected performance parameters.

Keywords

Doubly fed induction machine, Wind Power, Bidirectional Converter, Backsteeping control, vector control, Maximum Power Point Tracking (MPPT).

1. INTRODUCTION

Increasing of environmental awareness, conservation of natural resources, increase of fossil fuels prices and the continuous search of lowering energy dependency on fossil fuels have encouraged the development of directives and national legislations enabling the deployment of new energy generation technologies such as renewable energy sources (RES). In addition, the energy's demand has been increased worldwide and it will continue to grow while fossil fuels are seeing rapid depletion which has motivated to look toward the deployment of more alternative energy sources. On the other hand, the new paradigm of distributed generation (DG) has led to a new trend of non-centralized energy production close to the end users by using renewable energies sources such as photovoltaic systems, wind turbines and other non-conventional sources and their integration into the distribution network forming a localized micro grid [1], [2] and [3].The wind energy has gained a high level of interest in recent years, mainly because is one of the most efficient forms of renewable energies all over the world [4], [5] and [6]. In 2007, an additional of almost 20,000 MW wind power was installed all over the world to reach 94,112 MW of the overall installed capacity. Indeed this represents an increase of 31% compared with the 2006 installed capacity and 27% compared with the global installed capacity [7] and [8].

Doubly-Fed Induction Generator (DFIG) is one of the most widely used generators of wind energy applications with more than 50% of installed Wind Energy Conversion Systems (WECS) using the variable speed technology [9] and [10]. Actually, DFIG presents noticeable advantages such as: variable speed generation, decoupled control of active and reactive powers, reduction of mechanical stresses and acoustic noise, improvement of power quality, maximum power capture capabilities and the use of a reduced power converter with a rated power of 25% of the total system power [11] and [12].

Backstepping is a recursive procedure which breaks a design problem for the overall system into a sequence of design problem for lower order system. In addition backstepping design does not force the designed system to appear linear, which can avoid cancellations of useful nonlinearities. Furthermore, additionally nonlinear damping terms can be introduced in feedback loop to enhance robustness [13], [14] and [15]. Motivated by these features of backstepping in one hand and on the other hand the high complexity and nonlinearity of wind energy conversion system, a control strategy based on this concept will be more appropriate in order to achieve the following performances:

* Performing mouth and rapid transient response of the injected power into the grid for stability purpose of the entire power system.
* Performing good and accurate tracking capabilities in steady state of both active and reactive reference powers injected into the grid utility.

This paper suggests a hybrid vector and backstepping control strategy applied to a DFIG wind energy system. The proposed control strategy finds its strong justification for its insensitivity to parameters variation and the stability of the output variables due to the use of Lyapunov conditions. Mainly, this technique enables to control independently the active and reactive generated powers by DFIG.

The rest of the paper is structured as follow. Section 2, briefly provides the models of different wind energy system components. In Section 3, vector control of both active and reactive power generation are derived while in section 4 a hybrid vector control and backstepping control applied to the whole system model is given. In Section 5, simulation results using Matlab/Simulink ™ are presented and discussed. Finally, conclusions of the present work are drawn.

2. MODELLING AND CONTROL OF THE INDIVIDUAL COMPONENTS OF WIND SYSTEM

The studied wind system based on DFIG is mainly composed of a wind turbine, doubly fed induction generator and bidirectional power converter. A model of each sub-system is given in Figure 1.

  ISSN: 1743-9310

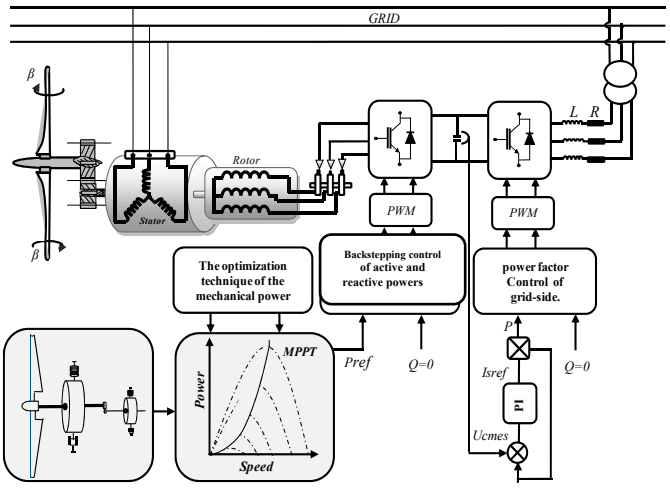

Fig. 1: Global configuration of the wind energy conversion system.

2.1 Modeling and Control of the Turbine

The turbine is made up of three-bladed rotor and a hub. Through the turbine, wind energy is transformed into mechanical energy that rotates the main shaft of the generator. The aerodynamic (mechanical) power P_m extracted by the wind turbine is given by [16]:

$$P_m = \frac{1}{2}.\rho.\pi.R_T^2.V^3.C_p(\lambda,\beta) \quad (1)$$

Where ρ is the air density, R_T is the wind turbine rotor length, V is the wind speed. The power coefficient $Cp\ (\lambda, \beta)$ represents the turbine efficiency to convert the kinetic energy of the wind into mechanical energy. This coefficient is a function of the blade pitch angle β and the tip speed ratio λ, which is defined as [17]:

$$\lambda = \frac{\Omega_T.R_T}{V} \quad (2)$$

where Ω_T is the shaft speed in (*rad/s*).
As a matter of example, the expression of the power coefficient of a wind turbine of *4Kw* is approximated using the following equation:

$$C_p(\lambda,\beta)=(0{,}5-0{,}167.(\beta-2)).\sin\left[\frac{\pi.(\lambda+0{,}1)}{18{,}5-0{,}3.(\beta-2)}\right]-0{,}00184.(\lambda-3).(\beta-2) \quad (3)$$

Figure 2 shows the plot of $Cp\ (\lambda,\beta)$ as a function of lambda and beta.

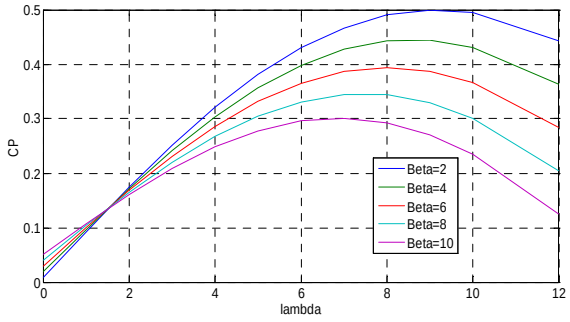

Fig. 2: Power coefficient *Cp* as a function of for different .

$$C_g = \frac{C_T}{G}, \qquad \Omega_T = \frac{\Omega_g}{G},$$

$$\frac{C_T}{G} - C_g = J.\frac{d\,\Omega_g}{dt} + f.\Omega_g \quad (4)$$

Ideal characteristics of a wind turbine at variable speed are enumerated below:

- Zone I: corresponds to the low speed where wind is insufficient to actuate the wind system. The objective in this zone is to extract the maximum power of the wind by applying techniques called extraction of maximum power.
- Zone II: In this zone, the speed of the wind is constant.
- Zone III: corresponds to the very high speed of the wind. The objective in this zone is to limit the output power to the nominal power of the wind system to avoid overloads. This is done by action on the pitch angle of the blades [18].

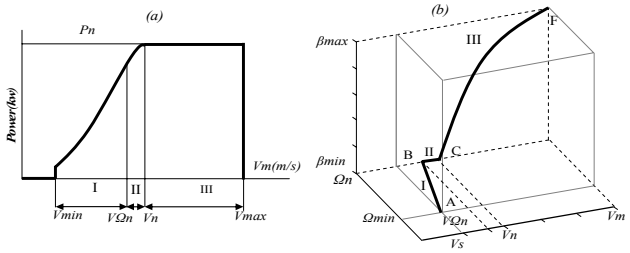

Fig. 3: Ideal characteristic of a wind turbine at variable speed.

Power optimization below the nominal output power zone

In this zone of operation, the control has as main objective to maximize the captured energy of the wind and to minimize the efforts undergone by the driving mechanism. To maximize the capture of wind energy, there are two variables which are controlled in order to be maintained at their optimal values namely: *λopt, βopt*. *β* is maintained by fixing the pitch angle at its optimal value *βopt*, and *λ* by fixing the specific speed to its optimal value. The corresponding characteristic to this relation is given in Zone I, Fig. 3.

Indirect control in Zone I

Optimization technique of the mechanical power used in this zone is the Maximum Power Point Tracking Control (MPPT). In the present work, the maximum power coefficient is taken as: *Cp max=0.48* by achieving for a tip speed ratio of *λopt =9.2* and *β=2* deg. This choice has been dictated according to Figure 2, [19].

$$C_{Topt} = \frac{1}{2}.\rho.\pi.R_T^3.V^2.\frac{C_p(\lambda_{opt})}{\lambda_{opt}} \quad (5)$$

$$V = \frac{R_T.\Omega_T}{\lambda_{opt}} \quad (6)$$

$$C_{Topt} = \frac{1}{2}.\rho.\pi.R_T^5.\frac{C_p(\lambda_{opt})}{\lambda_{opt}^3}.\Omega_T^2 \quad (7)$$

$$C_{Topt} = k_{opt}.\Omega_T^2 \quad and \quad k_{opt} = \frac{1}{2}.\rho.\pi.R_T^5.\frac{C_p(\lambda_{opt})}{\lambda_{opt}^3}$$

$$\frac{C_T}{G} - C_g - f.\Omega_g = 0 \quad and \quad \frac{k_{opt}}{G}.\Omega_T^2 - f.\Omega_g - C_g = 0$$

 ISSN: 1743-9310

with: $\Omega_g = G.\Omega_T$ then $C_{gopt} = \frac{k_{opt}}{G^3}.\Omega_g^2 - f.\Omega_g$

The block diagram given by Figure 4 shows the implementation of the indirect control of the turbine.

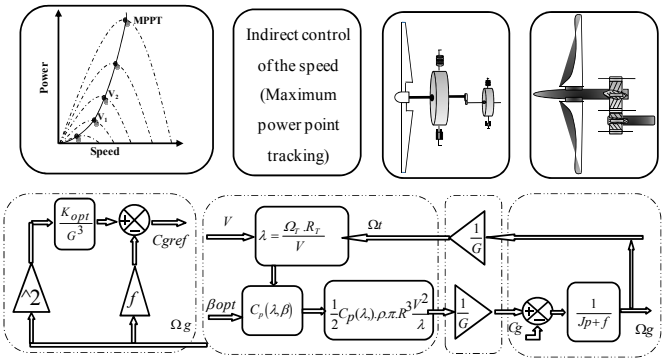

Fig. 4: Block diagram of the turbine and indirect control speed.

2.2 Generator Model

Classical modeling of the doubly fed induction generator in the Park reference frame is used. Voltage and flux equations of the DFIG are provided as follow [20], [21], [22] and [23]:

$$\begin{cases} V_{sd} = R_s I_{sd} + \frac{d\varphi_{sd}}{dt} - w_s \varphi_{sq} \\ V_{sq} = R_s I_{sq} + \frac{d\varphi_{sq}}{dt} + w_s \varphi_{sd} \\ V_{rd} = R_r I_{rd} + \frac{d\varphi_{rd}}{dt} - w_r \varphi_{rq} \\ V_{rq} = R_r I_{rq} + \frac{d\varphi_{rq}}{dt} + w_r \varphi_{rd} \end{cases} \quad and \quad \begin{cases} \varphi_{sd} = L_s I_{sd} + M I_{rd} \\ \varphi_{sq} = L_s I_{sq} + M I_{rq} \\ \varphi_{rd} = L_r I_{rd} + M I_{sd} \\ \varphi_{rq} = L_r I_{rq} + M I_{sq} \end{cases} \tag{8}$$

Electromagnetic torque equation is given by:

$$C_{em} = p\frac{M}{L_s}\left(I_{rd}\varphi_{sq} - I_{rq}\varphi_{sd}\right) \tag{9}$$

Stator active and reactive powers are expressed by:

$$\begin{cases} P = V_{sd} I_{sd} + V_{sq} I_{sq} \\ Q = V_{sq} I_{sd} - V_{sd} I_{sq} \end{cases} \tag{10}$$

In the state space representation, the system is given as:

$$[\dot{X}] = [A].[X] + [B].[U] \tag{11}$$

with:

$$[X] = \left[\varphi_{sd} \quad \varphi_{sq} \quad i_{rd} \quad i_{rq}\right]^t; \quad [U] = \left[v_{sd} \quad v_{sq} \quad v_{rd} \quad v_{rq}\right]^t;$$

where:

$$[A] = \begin{bmatrix} \frac{-1}{T_s} & w_s & \frac{M}{T_s} & 0 \\ -w_s & \frac{-1}{T_s} & 0 & \frac{M}{T_s} \\ \alpha & -\beta w_e & -\delta & w_r \\ \beta w_e & \alpha & -w_r & -\delta \end{bmatrix}; \quad [B] = \begin{bmatrix} 1 & 0 & 0 & 0 \\ 0 & 1 & 0 & 0 \\ \frac{-M}{\sigma L_r L_s} & 0 & \frac{1}{\sigma L_r} & 0 \\ 0 & \frac{-M}{\sigma L_r L_s} & 0 & \frac{1}{\sigma L_r} \end{bmatrix};$$

α, β and δ are constants defined as follows:

$$\alpha = \frac{M}{\sigma T_s L_s L_r}; \qquad \beta = \frac{M}{\sigma L_s L_r};$$

$$\delta = \frac{1}{\sigma}\left(\frac{1}{T_r} + \frac{M^2}{T_s L_r L_s}\right); \quad w_e = w_s - w_r$$

2.3 Modeling and control of the Grid side converter

The Grid side converter is used to provide bi-directed power flow from rotor-side converter allowing the stabilization of the DC-link voltage and achieving unity power factor.

Grid side converter modelling

The AC source model and the rectifier model are given by the state space representation:

$$\frac{d}{dt}\begin{bmatrix} i_1 \\ i_2 \\ i_3 \end{bmatrix} = \begin{bmatrix} -\frac{R}{L} & 0 & 0 \\ 0 & -\frac{R}{L} & 0 \\ 0 & 0 & -\frac{R}{L} \end{bmatrix}\begin{bmatrix} i_1 \\ i_2 \\ i_3 \end{bmatrix} + \frac{1}{L}\begin{bmatrix} V_1 - V_{an} \\ V_2 - V_{bn} \\ V_3 - V_{cn} \end{bmatrix} \tag{12}$$

The converter:

$$\begin{bmatrix} V_A \\ V_B \\ V_C \end{bmatrix} = \frac{Uc}{3}.\begin{bmatrix} 2 & -1 & -1 \\ -1 & 2 & -1 \\ -1 & -1 & 2 \end{bmatrix}\begin{bmatrix} S_1 \\ S_2 \\ S_3 \end{bmatrix} \tag{13}$$

In addition, the rectified current is given by:

$$i_s = \begin{bmatrix} S_1 & S_2 & S_3 \end{bmatrix}\begin{bmatrix} i_1 \\ i_2 \\ i_3 \end{bmatrix} \tag{14}$$

The output voltage is governed by:

$$\frac{dU_C}{dt} = \frac{1}{C}\left(i_s - i_L\right) \tag{15}$$

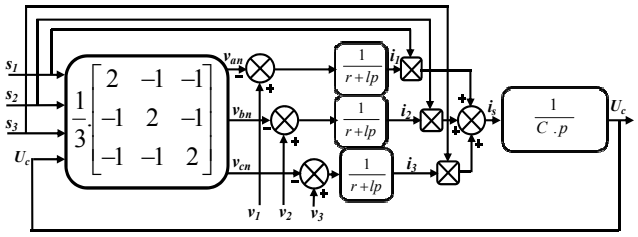

Fig.5: Schematic diagram of grid side converter.

Grid side converter controller design

The objective of the grid side converter is to regulate the DC link voltage and to set a unity power factor. The equations allowing the expression of the input AC voltage *Vp(d,q)* to the rectifier in the (*d,q*) frame as a function of the voltages at the common connection point *(CCP), V(d,q)* are given by the following equations:

$$\begin{cases} V_{pd} = V_d - R.i_d - L\frac{di_d}{dt} + Lw.I_q \\ V_{pq} = V_q - R.i_q - L\frac{di_q}{dt} - Lw.I_d \end{cases} \tag{16}$$

 ISSN: 1743-9310

The real and reactive powers are expressed by:

$$\begin{cases} P = \frac{3}{2}\left[V_d I_d + V_q I_q\right] \\ Q = \frac{3}{2}\left[V_q I_d + V_d I_q\right] \end{cases} \quad (17)$$

which can be rewritten in grouped form as follows:

$$\begin{bmatrix} P \\ Q \end{bmatrix} = \frac{3}{2}\cdot\begin{bmatrix} V_d & V_q \\ V_q & -V_d \end{bmatrix}\begin{bmatrix} I_d \\ I_q \end{bmatrix} \quad (18)$$

Equation (19) allows processing the reference currents (I^*_d , I^*_q) knowing the active and reactive powers references (P^* , Q^*).

$$\begin{bmatrix} I^*_d \\ I^*_q \end{bmatrix} = \frac{2}{3\left(V_d{}^2 + Vq^2\right)}\begin{bmatrix} V_d & V_q \\ V_q & -V_d \end{bmatrix}\begin{bmatrix} P^* \\ Q^* \end{bmatrix} \quad (19)$$

where V_d, V_q are the actual measured grid voltages.

The reference of the real power P^* is calculated from the DC bus control loop responsible of maintaining constant DC capacitor voltage. Its value is given by the following expression:

$$P^* = U_c I_s \quad and \quad Q^* = 0$$

The block diagram of the regulation is represented in Figure 6.

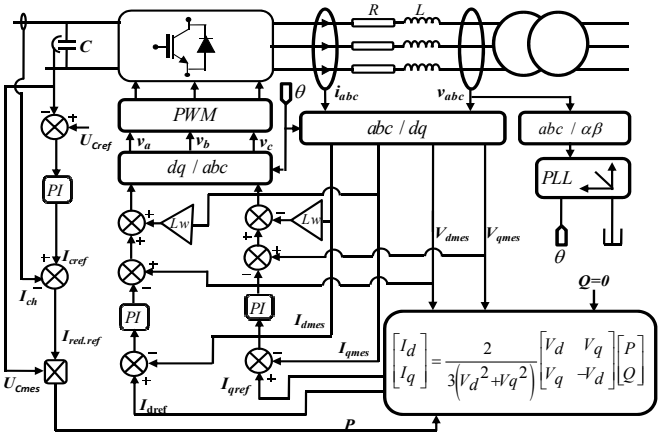

Fig.6: Block diagram of the grid side converter control.

2.4 Rotor side converter modeling

Rotor side converter is used to control the active and reactive powers injected by the stator of the doubly fed induction generator to the grid. The used converter is a simple two levels three-phase inverter (Fig.7).

The mathematical model of the rotor side converter is given by:

$$\begin{bmatrix} V_A \\ V_B \\ V_C \end{bmatrix} = \frac{E}{6}\cdot\begin{bmatrix} 2 & -1 & -1 \\ -1 & 2 & -1 \\ -1 & -1 & 2 \end{bmatrix}\begin{bmatrix} S_1 \\ S_2 \\ S_3 \end{bmatrix} \quad (20)$$

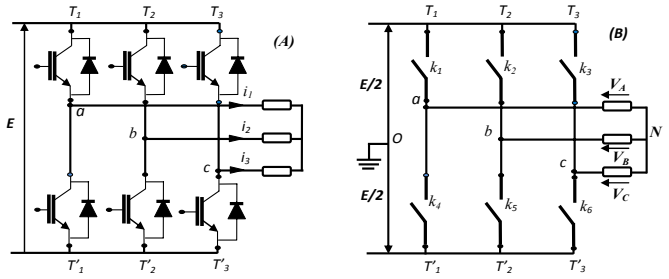

Fig.7: Schematic diagram of the rotor side converter.

3. VECTOR CONTROL OF ACTIVE AND REACTIVE POWER

Vector control allows independently control the flow of active and reactive powers between the grid and generator [24].

Stator and rotor variables are both referred to the stator reference park frame. Using this orientation, the *d*-component of the stator flux is equal to the total flux whereas the *q*-component of the stator flux is zero: $\varphi_{sd}=\varphi_s$ and $\varphi_{sq}=0$. With this approach, decoupled control between active and reactive powers of the stator is obtained [25].

Assuming that the resistance of the stator windings (*Rs*) is neglected and referring to the chosen reference frame chosen, the voltage and the flux equations of the stator winding can be simplified in steady state as follow [26]:

$$\begin{cases} V_{sd} = 0 \\ V_{sq} = V_s = w_s.\varphi_s \\ V_{rd} = R_r.I_{rd} + \frac{d\varphi_{rd}}{dt} - w_r\varphi_{rq} \\ V_{rq} = R_r.I_{rq} + \frac{d\varphi_{rq}}{dt} + w_r\varphi_{rd} \end{cases} \quad (21)$$

The equations of flux are expressed by:

$$\begin{cases} \varphi_{sd} = \varphi_s = L_s.I_{sd} + M.I_{rd} \\ 0 = L_s.I_{sq} + M.\varphi_{rq}. \\ \varphi_{rd} = L_r.I_{rd} + M.\varphi_{sd}. \\ \varphi_{rq} = L_r.I_{rq} + M.\varphi_{sq}. \end{cases} \quad (22)$$

The relationship between stator powers and rotor currents are given by the following equations:

$$\begin{cases} P_s = -\frac{V_s.M}{L_s}.I_{rq} \\ Q_s = \frac{V_s{}^2}{w_s.L_s} - \frac{V_s.M}{L_s}.I_{rd} \end{cases} \quad (23), \quad \begin{cases} I_{rq} = -\frac{L_s}{V_s.M}.P_s \\ I_{rd} = \frac{V_s{}^2}{w_s.L_s} - \frac{L_s}{V_s.M}.Q_s \end{cases} \quad (24)$$

The obtained control voltages which will drive the rotor are given using the following expressions:

 ISSN: 1743-9310

$$\begin{cases} V_{rd} = \left[R_r + \left(L_r - \dfrac{M^2}{L_s} \right) s \right] I_{rd} - g w_s \left(L_r - \dfrac{M^2}{L_s} \right) . I_{rq} \\ V_{rq} = \left[R_r + \left(L_r - \dfrac{M^2}{L_s} \right) s \right] I_{rq} + g w_s \left(L_r - \dfrac{M^2}{L_s} \right) . I_{rd} + g . \dfrac{V_s . M}{L_s} \end{cases} \quad (25)$$

In Figure 8, it is given the block diagram of vector control approach applied to the DIFG.

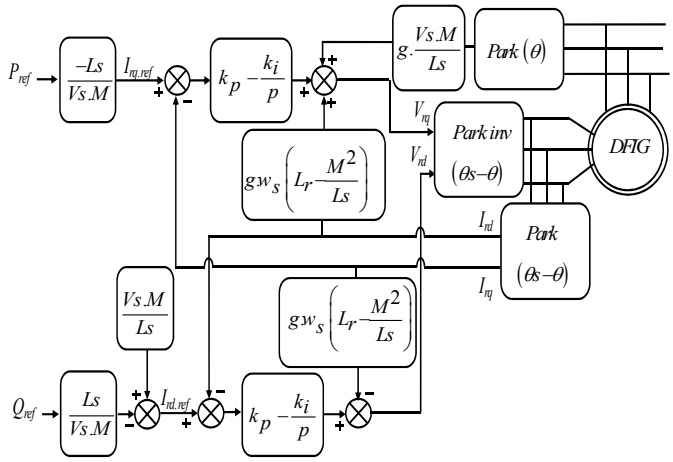

Fig.8: Block diagram of the vector control of the DFIG.

4. BACKSTEPPING CONTROL OF ACTIVE AND REACTIVE POWERS

Backstepping approach is a nonlinear technique widely used in the control design. The multiple advantages of this approach include its large set of globally and asymptotically stabilizing control laws and its capability to improve robustness and solve adaptive problems [27], and [28]. The basic idea of Backstepping control design is the use of the so-called "virtual control" to systematically decompose a complex nonlinear control design problem into simpler and smaller ones. Backstepping control design is divided into various design steps. Each step deals with a single input–single-output design problem, and each step provides a reference for the next design step. The overall stability and performance are achieved by Lyapunov theory for the whole system [29], [30], [31] and [32].

The backstepping control possesses strengthen robustness and has been successfully applied in wind energy conversion system. In this paper, a controller is designed for decoupled control of active and reactive powers based on the backstepping algorithm to match the variable environment of WECS.

The backstepping approach, which is based on the principle of vector control, will be applied to the control of the DFIG. In this case the control will be applied in the (*d, q*) reference by considering the orientation of the stator flux:

$$\begin{cases} \varphi_{sd} = \varphi_s \\ \varphi_{sq} = 0 \end{cases} \quad (26)$$

Equations of the derivative rotor currents are given by:

$$\begin{cases} \dfrac{dI_{rd}}{dt} = \left(V_{rd} - R_r . I_{rd} + g . w_s . L_r . \sigma . I_{rq} \right) . \dfrac{1}{L_r \sigma} \\ \dfrac{dI_{rq}}{dt} = \left(V_{rq} - R_r . I_{rq} - g . w_s . L_r . \sigma . I_{rd} - g . w_s . \dfrac{M . V_s}{w_s . L_s} \right) . \dfrac{1}{L_r \sigma} \end{cases} \quad (27)$$

Relations between stator powers and rotor currents are:

$$\begin{cases} I_{rq}^{ref} = -\dfrac{L_s}{V_s . M} . P_s^{ref} \\ I_{rd}^{ref} = \dfrac{V_s}{w_s . M} - \dfrac{L_s}{V_s . M} . Q_s^{ref} \end{cases} \quad (28)$$

Equations of the derivative rotor reference currents are:

$$\begin{cases} \dot{I}_{rq}^{ref} = -\dfrac{L_s}{V_s . M} . \dot{P}_s^{ref} \\ \dot{I}_{rd}^{ref} = -\dfrac{L_s}{V_s . M} . \dot{Q}_s^{ref} \end{cases} \quad (29)$$

4.1 Application of Backstepping control to DFIG

The combination of vector control and backstepping allow removing the PI regulators in vector control by Backstepping. Calculating of the control voltages is based on Lyapunov functions. This control is based on two steps which are given as follow:

Step 1:

In this step the errors" $\boldsymbol{E_1}$ "and "$\boldsymbol{E_2}$ ", which represent the error between the real currents $\left(I_{rd}, I_{rq} \right)$ and reference currents $\left(I_{rq}^{ref}, I_{rd}^{ref} \right)$, are identified.

$$\begin{cases} E_1 = \left(I_{rq}^{ref} - I_{rq} \right) \\ E_2 = \left(I_{rd}^{ref} - I_{rd} \right) \end{cases} \quad (30)$$

The derivative of these errors is given by:

$$\begin{cases} \dot{E}_1 = \left(\dot{I}_{rq}^{ref} - \dot{I}_{rq} \right) \\ \dot{E}_2 = \left(\dot{I}_{rd}^{ref} - \dot{I}_{rd} \right) \end{cases} \quad (31)$$

The Lyapunov function is defined by:

$$v = \frac{1}{2} \left(E_1^2 - E_2^2 \right) \quad (32)$$

To make the derivative of the Lyapunov function becomes null, one must choose errors as follows:

$$\dot{E}_1 = -k_1 . E_1 \qquad \text{and} \qquad \dot{E}_2 = -k_2 . E_2$$

Time derivative of the Lyapunov function is:

 ISSN: 1743-9310

$$\dot{V} = -k_1 E_1^2 - k_2 E_2^2 \prec 0 \quad (33)$$

with $k_1 \succ 0$ and $k_2 \succ 0$

By replacing the derivatives of the currents $\dot{I}_{rq}^{ref}$ and $\dot{I}_{rq}$ by their values, we get the expression of the derivative errors given by:

$$\begin{cases} \dot{E}_1 = \left(\left(-\frac{L_s}{MV_s} \dot{P}_s^{ref} \right) - \frac{1}{L_r \sigma} \left(V_{rq} - R_r I_{rq} - g w_s L_r \sigma I_{rd} - g \frac{MV_s}{L_s} \right) \right) \\ \dot{E}_2 = \left(\left(-\frac{L_s}{V_s M} \dot{Q}_s^{ref} \right) - \frac{1}{L_r \sigma} \left(V_{rd} - R_r I_{rd} + g w_s L_r \sigma I_{rq} \right) \right) \end{cases} \quad (34)$$

$$\begin{cases} \dot{E}_1 = \left(\left(-\frac{L_s}{MV_s} \dot{P}_s^{ref} \right) - \frac{1}{L_r \sigma} V_{rq} - \frac{1}{L_r \sigma} \left(-R_r I_{rq} - g w_s L_r \sigma I_{rd} - g \frac{MV_s}{L_s} \right) \right) \\ \dot{E}_2 = \left(\left(-\frac{L_s}{V_s M} \dot{Q}_s^{ref} \right) - \frac{1}{L_r \sigma} V_{rd} - \frac{1}{L_r \sigma} \left(-R_r I_{rd} + g w_s L_r \sigma I_{rq} \right) \right) \end{cases} \quad (35)$$

Step 2:

By replacing the derivatives of the error by their values, we obtain:

$$\begin{cases} -k_1 E_1 = \left(\left(-\frac{L_s}{MV_s} \dot{P}_s^{ref} \right) - \frac{1}{L_r \sigma} V_{rq} - \frac{1}{L_r \sigma} \left(-R_r I_{rq} - g w_s L_r \sigma I_{rd} - g \frac{MV_s}{L_s} \right) \right) \\ -k_2 E_2 = \left(\left(-\frac{L_s}{V_s M} \dot{Q}_s^{ref} \right) - \frac{1}{L_r \sigma} V_{rd} - \frac{1}{L_r \sigma} \left(-R_r I_{rd} + g w_s L_r \sigma I_{rq} \right) \right) \end{cases} \quad (36)$$

Finally the choice of the control law is as follows:

$$\begin{cases} V_{rq} = \left(L_r \sigma \left(-\frac{L_s}{MV_s} \dot{P}_s^{ref} + k_1 E_1 \right) + R_r I_{rq} + g w_s L_r \sigma I_{rd} + g \frac{MV_s}{L_s} \right) \\ V_{rd} = \left(L_r \sigma \left(-\frac{L_s}{V_s M} \dot{Q}_s^{ref} + k_2 E_2 \right) + R_r I_{rd} - g w_s L_r \sigma I_{rq} \right) \end{cases} \quad (37)$$

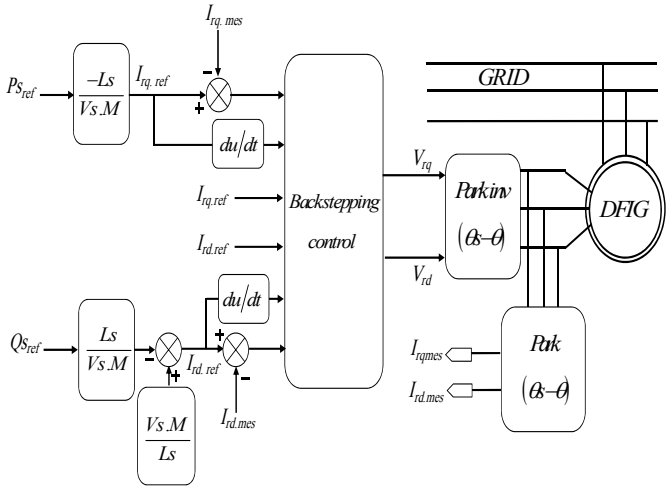

Fig.9: Block diagram of the Backstepping control.

5. SIMULATION RESULTS

5.1 Simulation results with fixed speed (without turbine)

In this case, remarkable improvements of dynamic and static performances are achieved by backstepping control approach compared to those obtained by PI regulator. Furthermore, this technique made possible a perfect decoupling between the two components of the stator's generated powers. Improvements are noticed in both transient and reference tracking mode. It is clearly shown (Fig. 10. b and 11.b) the dramatic amplitude reduction of the oxillations and almost zero error reference tracking in the case backstepping control.

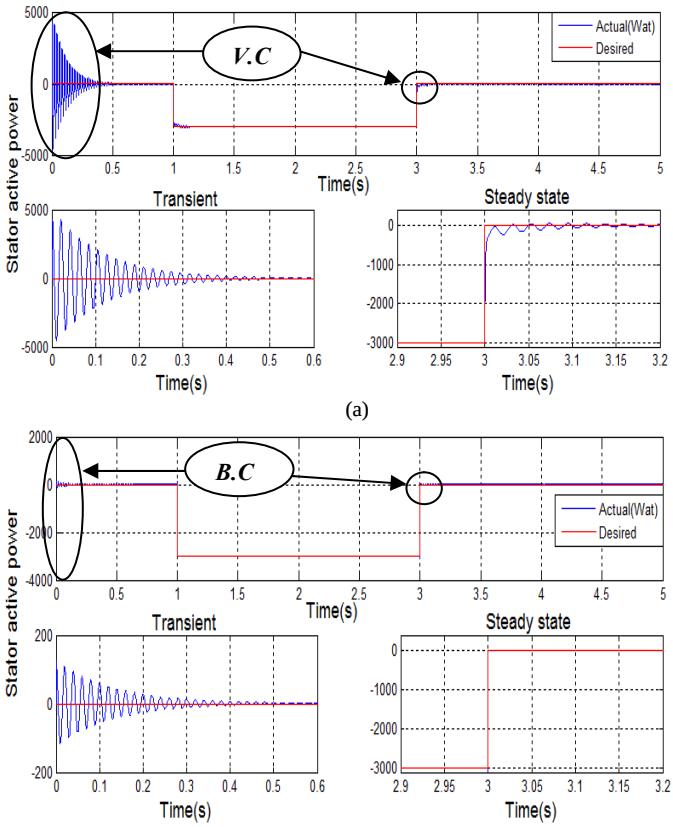

(a)

(b)

Fig. 10: Stator active power, (a): Vector control, (b): Backstepping control

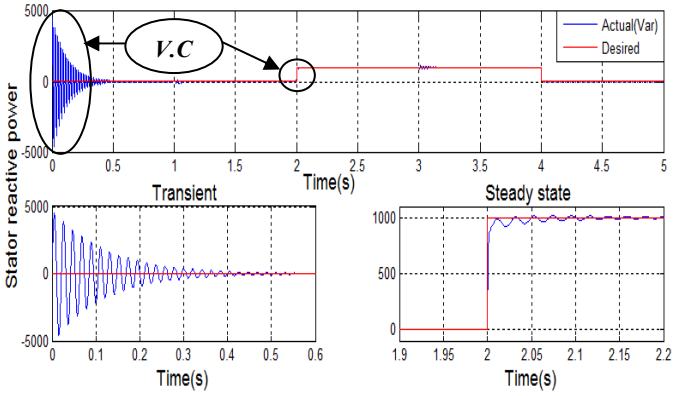

(a)

 ISSN: 1743-9310

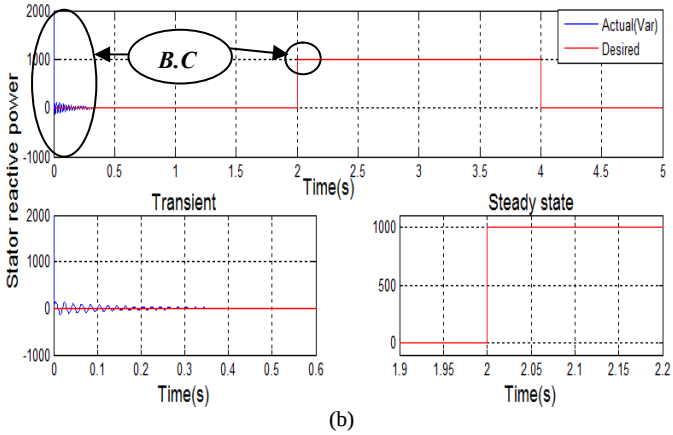

(b)

Fig. 11: Stator reactive power, (a): Vector control, (b): Backstepping control.

5.2 Results with turbine (variable speed)

Simulation results, given in Figures below show the performances of Backstepping control approach against those obtained by applying vector control to a wind turbine system formed by a cascaded DFIG, rectifier and a two level three phase inverter drawn by wind turbine.

The stator's active power reference set point is determined by the available power at the turbine stage. It shows clearly good tracking capabilities of the reference set point for both active and reactive powers by the DFIG. Fig.12. a, b and Fig.13. c, d show the wind profile used for simulation purpose, mechanical speed, power coefficient and tip-speed ratio respectively. Time variation of stator's active and reactive powers are shown in Fig.14.Currents through the stator, amplitude and frequency of rotor's currents are shown in Fig. 15 and 16 respectively. From these simulations, it is clearly shown in Fig. 17, the good tracking capabilities of the controller seen in the time evolution of the direct voltage. It is clearly.

In addition, one phase voltage and its current simulated are shown in Fig. 18 when DFIG operates at sub-synchronous state. Near unity power factor is also achieved confirming the ability of the pulse width modulation (PWM) rectifier to reduce harmonic contents. Control strategy approach using backstepping allows fast transient response and a near zero steady state error.

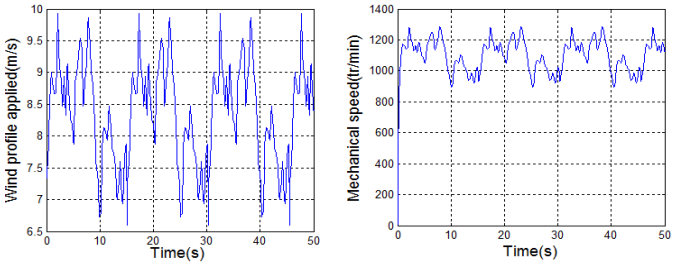

(a) (b)

Fig. 12: (a): Wind profil applied, (b): Mechanical speed.

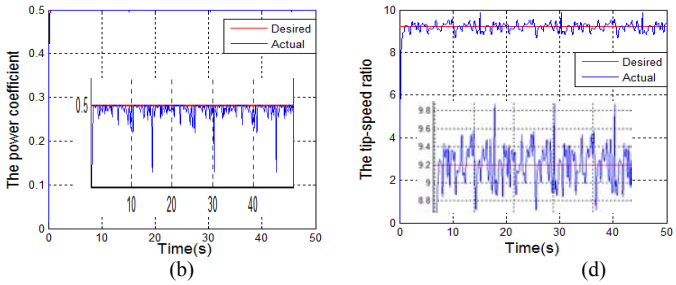

(b) (d)

Fig. 13: (c): Power coefficient, (d): Tip-speed ratio.

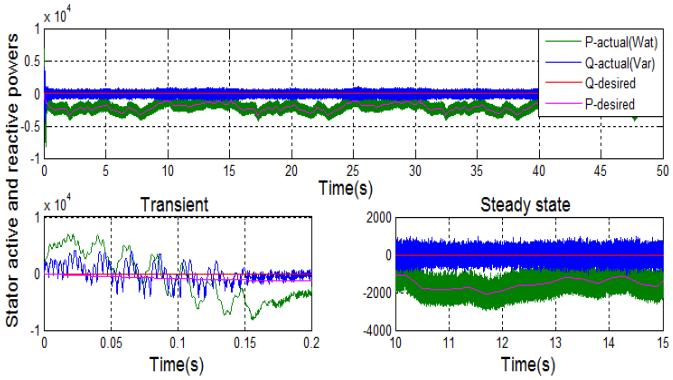

(a)

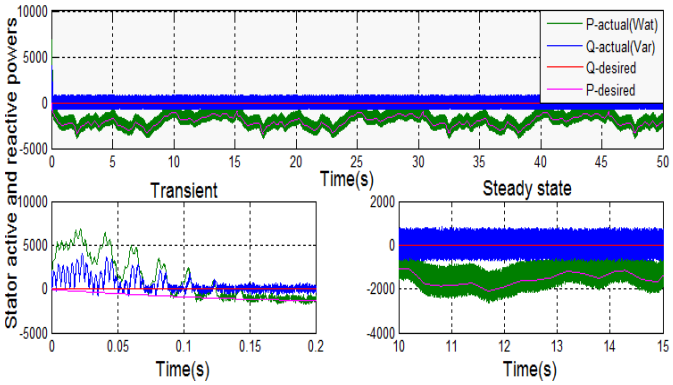

(b)

Fig. 14: (a): Stator's active and reactive powers, (a): Vector control, (b): Backstepping control.

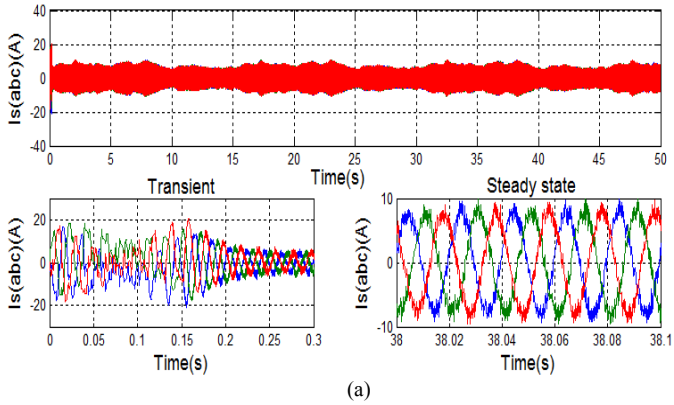

(a)

 ISSN: 1743-9310

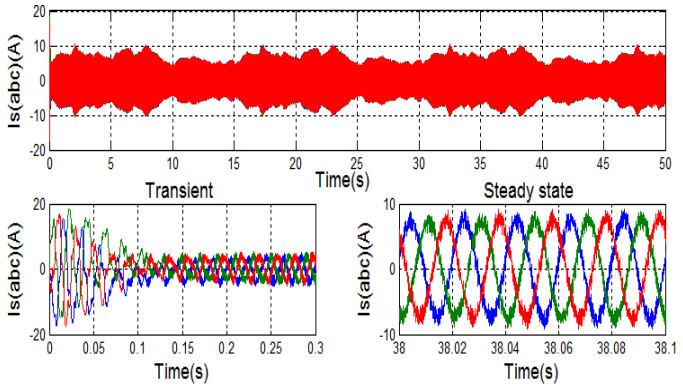

(b)

Fig.15: Stator current components, (a): Vector control, (b): Backstepping control.

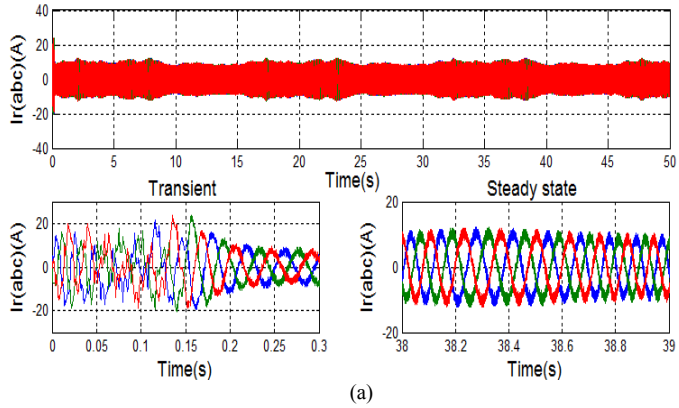

(a)

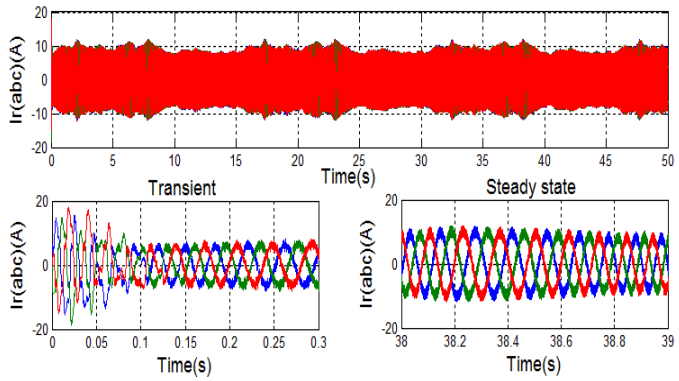

(b)

Fig.16: Rotor current components, (a): Vector control, (b): Backstepping control.

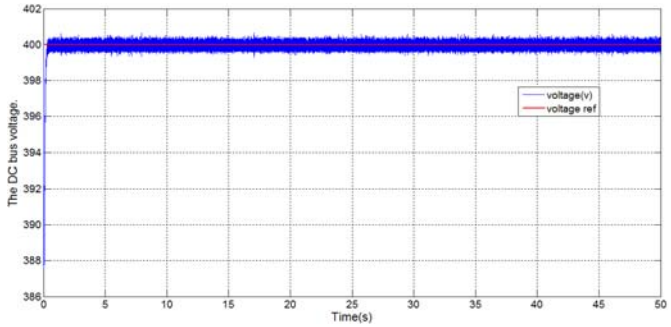

Fig.17: DC bus voltage.

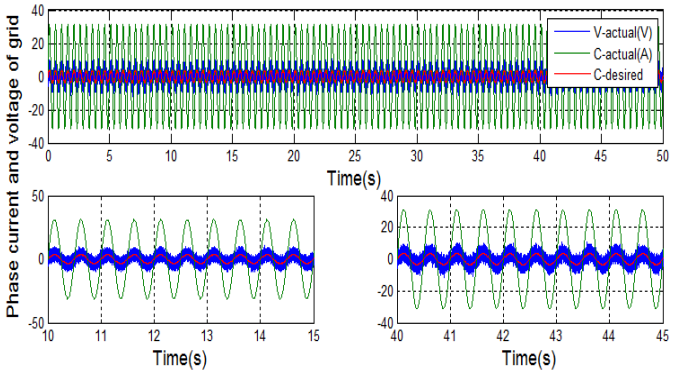

Fig.18: The phase current and voltage of the grid.

6. CONCLUSION

The actual paper presents a comparative study on the performance of two control strategies: PI based and Backstepping control approaches for DFIG wind turbine when operating in power regulation mode. Both approaches achieve by an appropriate control the direct and quadrature components of the rotor voltage, performed by the rotor side power converter, Backstepping controller is applied to decoupled control of the active and reactive powers for doubly fed induction generator and show better performances in both transient and steady state. The designed controller is based on the stability theory of Lyapunov to ensure the stability and achieve the expected control results. Simulation results show the decoupled control of both active and reactive powers and then are regulated separately. Thus, wind energy conversion systems with doubly fed induction generator can not only capture the maximum wind power, but also provide reactive power to meet the need of the utility grid with simplified controller structure.

7. APPENDIX

V_x	voltage
I	current
φ	flux linkage
Ω_n	nominal value of angular rotor speed
Rs	stator resistance
Rr	rotor resistance
M	mutual inductance
Ls	stator inductances
Lr	rotor inductances
σ	total leakage factor
J	moment of inertia
P	number of pole pairs
C_e	electromagnetic torque
C_T	turbine torque
C_g	generator torque
Ω_T	turbine speed
Ω_g	generator speed
θs	rotor flux position
ωr	electrical angular rotor speed
ωs	synchronously rotating angular speed
ρ	air density
R_T	radius of turbine
Cp	power coefficient
λ	speed ratio
β	pitch angle

 ISSN: 1743-9310

E	error
X^{ref}	reference value of x
$Xopt$	optimal value of x
d,q	park reference frame
AC	alternative current
DC	direct current
P	active power
Q	reactive power

8. REFERENCES

[1] R. Velik, P. Nicolay, "A cognitive decision agent architecture for optimal energy management of microgrids", Energy Conversion and Management, Vol. 8, 2014, pp. 831-847.

[2] M. Motevasel, A. R. Seifi, "Expert energy management of a micro-grid considering wind energy uncertainty", Energy Conversion and Management, Vol. 83, July 2014, pp. 58-72.

[3] K. Abdeladim, A. Hadj Arab, A. Chouder, F. Cherfa, S. Bouchakourand K. Kerkouche, "Contribution for Solar Mapping in Algeria", Chapter Book in Progress in Sustainable Energy Technologies, Springer International Publishing Switzerland Algiers, Algeria, 2014, pp. 439-447.

[4] Wen J, Zheng Y, Donghan F, "A review on reliability assessment for wind power", Renewable and Sustainable Energy Reviews, Vol. 13, Issue. 9, December 2009, pp. 2485-2494

[5] Hoogwijk M, De Vries B, Turkenburg W, "Assessment of the global and regional geographical, technical and economic potential of onshore wind energy", Energ Econ, Vol. 26, Issue. 5, September 2004, pp. 889-919.

[6] Fatma Hachicha, Lotfi Krichen, "Rotor power control in doubly fed induction generator wind turbine under grid faults", Energy, Vol. 44, Issue. 1, August 2012, pp. 853-861

[7] The Global Wind Energy Council, GWEC Latest News, 2008, US, China & Spain lead world wind power market in 2007, February, available at [http://www.gwec.net/], last date accessed: 2008.

[8] Hany M. Hasanien, S.M. Muyeen, "Speed control of grid-connected switched reluctance generator driven by variable speed wind turbine using adaptive neural network controller", Electrical Power and Energy Systems, Vol. 84, March 2012, pp. 206-213.

[9] M. Liserre, R. Cardenas, M. Molinas, J. Rodriguez, "Overview of multi-MW wind turbines and wind parks", IEEE Transactions on Industrial Electronics, Vol. 58, 2011, pp. 1081-1095.

[10] Roberto Cardenas, Ruben Pena, Patrick Wheeler, Jon Clare, Andres Munoz, Alvaro Sureda, "Control of a wind generation system based on a Brushless Doubly-Fed Induction Generator fed by a matrix converter", Electrical Power and Energy Systems, Vol. 103, October 2013, pp. 49-60.

[11] Fernando Valenciaga, "Second order sliding power control for a variable speed-constant frequency energy conversion system", Energy Conversion and Manage, Vol. 51, 2010, pp.3000-3008.

[12] Mohammad Farshadnia, Seyed Abbas Taher, "Current-based direct power control of a DFIG under unbalanced grid voltage", Electr Power Energy and Syst, Vol. 62, November 2014, pp.571–582.

[13] K. J. Astrom and B. Wittenmark, "Adaptive Control", New York: Addison Wesley, 1995

[14] Jeng-Dao Lee, Member, IEEE, Suiyang Khoo and Zhi-Bin Wang, "Backstepping-based Current and Voltage Control Strategy for Maglev Position Device", 2013 IEEE, pp. 3341-3346.

[15] M.Sharma, A.Verma, "Adaptive Tracking Control for a Class of Uncertain Non-Affine Delayed Systems Subjected to Input Constraints using Self Recurrent Wavelet Neural Network",Proc IEEE Conf. on Advances in Recent Technologies in Communication and Computing, Kottayam, 16-17 October 2010, pp.60-65.

[16] S.Abdeddaim, A.Betka, S Drid, M Becherif, "Implementation of MRAC controller of a DFIG based variable speed grid connected wind turbine", Energy Convers Manage, Vol. 79, March 2014, pp.281-288.

[17] M.L. Corradini, G. Ippoliti, and G. Orlando, "An Aerodynamic Torque Observer for the Robust Control of Variable-Speed Wind Turbines", Proc. 51st IEEE Conf. on Decision and Control, Maui, Hawaii, USA, 10-13 December 2012, pp. 2483-2488.

[18]F.D. Bianchi, H. De Battista, R.J. Mantz, "Wind turbine control systems, principles, Modelling and Gain Scheduling Design", Springer 2007.

[19] Radia Abdelli, DjamilaRekioua, ToufikRekioua, Abdelmounaïm Tounzi, "Improved direct torque control of an induction generator used in a wind conversion system connected to the grid", ISA Transactions, Vol. 52, Issue. 4, July 2013, pp. 525-538.

[20]T. Mesbahi, T. Ghennam, E.M. Berkouk, "A Doubly Fed Induction Generator for Wind Stand-Alone Power Applications (Simulation and Experimental Validation)", Proc. 2012 IEEE. International Conference Electrical Machines (ICEM), Marseille, 2-5 Sept 2012, pp. 2028-2033.

[21] Yongchang Zhang, Jianguo Zhu, Jiefeng Hu, "Model predictive Direct torque control for grid Synchronization of Doubly Fed Induction Generator", Proc. 2011 IEEE. International Electric Machines & Drives Conference (IEMDC), Niagara Falls, 15-18 May 2011, pp. 765-770.

[22]Victor Flores Mendes, Clodualdo Venicio de Sousa, Selˆenio Rocha Silva, Balduino Cezar Rabelo, Jr., and Wilfried Hofmann, Senior Member, IEEE. Modeling and Ride-Through, "Control of Doubly Fed Induction Generators During Symmetrical Voltage", Sags. IEEE Trans. Energy Convers, Vol. 26, No. 4, Dec 2011, pp. 1161-1171.

[23] Esmaeil Rezaei, AhmadrezaTabesh, Member, IEEE, and Mohammad Ebrahimi, "Dynamic Model and Control of DFIG Wind Energy Systems Based on Power Transfer Matrix", IEEE Trans. Energy Convers, Vol. 27, No. 3, july 2012, pp. 1485-1493.

[24] H.T. Jadhav, Ranjit Roy, "A comprehensive review on the grid integration of doubly fed induction generator", Int J Electr Power Energy Syst, Vol. 49, No. 1, july 2013, pp. 8–18.

[25] S. Abdeddaim, A. Betka, "Optimal tracking and robust power control of the DFIG wind turbine", Int J Electr Power Energy Syst Vol. 49, No. 1, july 2013, pp.234-242.

[26] K. Ghedamsi, E.M. Berkouk, "Control of wind generator associated to a flywheel energy storage system". Renewable Energy, Vol 33, Issue 9, Elsevier (2008), pp 2145-2156.

[27] Zhankui Song, Kaibiao Sun, "Adaptive backstepping sliding mode control with fuzzy monitoring strategy for a kind of mechanical system", ISA Transactions, Vol. 53, Issue. 1, January 2014, pp. 125-133.

[28] Amat Amir basari, yahya Md. Sam and Norhazimi Hamzah. "Nonlinear Active Suspension System with Backstepping Control Strategy", Proc. 2nd IEEE Conf. on Industrial Electronics and Applications, 2007, pp.554-558.

[29] Ramzi Trabelsi, Adel Khedher, Mouhamed Faouzi Mimouni, Faouzi M'sahli, "Backstepping control for an induction motor using an adaptive sliding rotor-flux observer", Electric Power Systems Research, Vol. 93, December 2012, pp.1-15.

[30] M.R Jovanovic, B. Bamieh, "Architecture Induced by Distributed Backstepping Design", IEEE Transactions on Automatic Control, Vol. 52, Issue. 1, January 2007, pp. 108-113.

[31] A. Laoufi, A. Hazzab, I.K. Bousserhane and M. Rahli, "Direct Field Oriented control using Backstepping technique for Induction Motor speed control", International Journal of Applied Engineering Research, Vol. 1, No l, 2006, pp. 37-50.

[32] Mourad Loucif, Abdelmadjid Boumediene and Abdelkader Mechernene, "Backstepping Control of Double Fed Induction Generator Driven by Wind Turbine", Proc. 3rd IEEE Conf. on Systems and Control, Algiers, Algeria, 29-31October 2013.

AUTHORS' BIOGRAPHIES

Mr. Riyadh Rouabhi was born in M'sila, Algeria. He received the M.Sc. degrees in Electrical Engineering from Ferhat Abbas University, Setif, Algeria, in 2012. He has been working for more than 4 years with the Department of Electrical Engineering, University of M'sila, as a Professor and Engineer laboratory. Currently. His current area of research includes design and control of doubly fed induction Generator, reliability, magnetic bearing, and renewable energy.

Pr. .Rachid Abdessemed was born in Batna, Algeria, . He received the M.Sc. and Ph.D. degrees in Electrical Engineering from Kiev Polytechnic Institute, Kiev, Ukraine, in 1978 and 1982; respectively. He has been working for more than 30 years with the Department of Electrical Engineering, University of Batna, as a Professor. Currently, he is the Director of the Electrical Engineering Laboratory. His current area of research includes design and control of induction machines, reliability, magnetic bearing, and renewable energy.

Dr. Aissa Chouder received the Ingénieur in Electronics and Magister in Electronics degrees from Ferhat Abbas University, Sétif, Algeria, in 1991 and 1999, respectively, and the Ph.D. degree in electronic engineering from the Universitat Politècnica de Catalunya (UPC), Barcelona, Spain, in 2010. He is currently a Senior Researcher with the Photovoltaic Laboratory, Development Centre of Renewable Energies, Algiers, Algeria. His research interests include power electronics modeling and control for renewable energy systems.

Dr. DJERIOUI was born in M'sila, Algeria, in 1986.In 2009,he received the engineering degree in electrical engineering from the University of M'sila, Algeria. In 2011,he was graduated M.Sc. degree in electrical engineering from the Polytechnic Military Academy in Algiers, Algeria respectively where he is currently working toward the Ph.D. degree in Electronic Instrumentation systems at the University of USTHB, Algiers, Algeria. His main interests are power converters, control and power quality.

  ISSN: 1743-9310